An Analytical Study of Laminar Counterflow Double-Pipe Heat Exchangers

RICHARD J. NUNGE
Syracuse University, Syracuse, New York

WILLIAM N. GILL
Clarkson College of Technology, Potsdam, New York

An orthogonal expansion technique for solving a new class of counterflow heat transfer problems is developed and applied to the detailed study of laminar flow concentric tube heat exchangers. The exchanger problem is solved for fully developed laminar velocity profiles, negligible longitudinal conduction in the fluid streams and in the exchanger walls, and with fluid properties which are independent of the temperature.

A description of the variation of the local Nusselt numbers and the temperature at the wall between the two streams is given. Also reported are bulk temperature changes in the two streams and mean overall Nusselt numbers. It is shown that for long exchangers, which are of some industrial importance, asymptotic Nusselt numbers exist in counterflow as in single-phase and cocurrent systems. Numerical values of asymptotic Nusselt numbers are reported for a wide range of parameters. Comparisons are made with single-stream solutions such as the Graetz problem, with empirical correlations of experimental data, and with cocurrent flow exchangers.

To solve this problem it was necessary to derive new orthogonality relations, and also expressions for determining positive and negative sets of eigenvalues and eigenvectors. Satisfaction of inlet boundary conditions at both ends of counterflow exchangers requires a complete set of eigenfunctions and thus one must use both the positive and negative sets.

Forced convection heat transfer in bounded conduits has received and continues to receive a great deal of attention in the literature. Theoretical studies are generally extensions of the classical Graetz problem of a fluid in fully developed laminar flow in a circular duct with a uniform wall temperature boundary condition. Extensions have been made to different geometries and to a variety of boundary conditions (*5, 14, 16*) in an attempt to simulate physical situations more closely.

Beyond the initial concern for the single-stream problem, it is natural to speculate on the applicability of these results to double-pipe heat exchangers which are used extensively in industrial applications. However, the question remains as to what type of condition exists at a wall between two streams in a practical heat exchanger. Stein (*17*) has recently answered this question in part by a further extension of the Graetz problem to cocurrent flow heat exchangers. However, a solution for the countercurrent flow problem does not follow readily from either the single-stream or the cocurrent problem because of two fundamental differences. First, as illustrated in Figures 1*a* and 1*b*, the velocity profile in single-stream and cocurrent flow problems is always positive or zero, while in countercurrent flow the velocity profile (Figure 1*c*) changes sign with respect to a fixed coordinate system. Second, in Figures 2*a* and 2*b*, both the single-stream and cocurrent systems are open-ended with respect to the specified boundary conditions, but the counterflow system is neither open-ended nor completely bounded, as shown in Figure 2*c*.

As a consequence of these differences the counterflow problem has at least two unique aspects:

1. It requires the development of new orthogonality relations for the sets of positive and negative eigenfunctions associated with positive and negative sets of eigenvalues.

2. Complete orthogonal expansions utilizing both sets of eigenfunctions must be written at both ends of the counterflow problem to satisfy inlet conditions. Therefore, it is necessary to find a new procedure for evaluating the eigenvectors, or expansion coefficients, associated with the complete set of orthogonal functions.

The purpose of this work is to apply an orthogonal expansion technique to a counterflow concentric tube heat exchanger, which is a system of industrial importance, and also to show that the method of analysis is applicable to a broad class of multistream heat and mass transfer problems which have not been solved in detail previously. The present work includes the effects of different fluid properties in the streams and a resistance to transfer between them which were not included in the initial analysis (*11*) of countercurrent systems.

In another paper (*12*), orthogonal expansion solutions for parallel plate exchangers were obtained. Since a rigorous proof of the method of solution used is not available, the problem was also solved by a finite-difference technique. It was found that the agreement in local behavior determined by the two methods was excellent. This is viewed as definitive justification for the validity of both methods of solving counterflow heat transfer problems, since it is very unlikely that such excellent agreement would be fortuitous.

THEORETICAL DEVELOPMENT

The system considered is shown schematically in Figure 3. A detailed description of the analysis of counterflow double-pipe heat exchangers, which includes Equations (1) through (40), is available elsewhere.* Only a very

Richard J. Nunge is with Clarkson College of Technology, Potsdam, New York.

* Equations (1) through (40) and (54) to (60) and Tables 1, 2, 4, 9 to 11 have been deposited as document 8678 with the American Documentation Institute, Photoduplication Service, Library of Congress, Washington 25, D. C., and may be obtained for $5.00 for photoprints or $2.25 for 35-mm. microfilm.

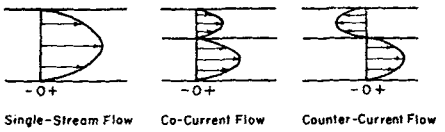

Fig. 1. Schematic diagrams of the velocity profiles in single-stream, cocurrent, and countercurrent flows.

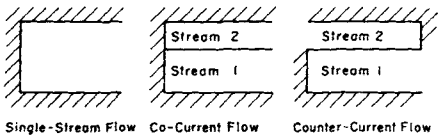

Fig. 2. Schematic diagrams of the boundary conditions for heat transfer in single-stream, cocurrent, and countercurrent flows.

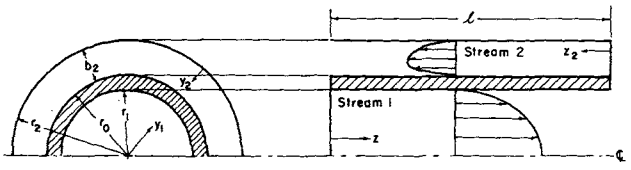

Fig. 3. Schematic diagram of the concentric tube heat exchanger.

brief summary which retains the same numbering system will be reported here. For fully developed laminar flow of fluids with no energy sources, constant but generally different fluid properties in each stream, and negligible longitudinal conduction, the energy equation in dimensionless form for the tube is

$$(1-y_1^2)\frac{\partial\theta_1}{\partial x}=\frac{1}{y_1}\frac{\partial}{\partial y_1}\left(y_1\frac{\partial\theta_1}{\partial y_1}\right);\qquad 0\leq y_1\leq 1,\quad 0\leq x\leq L \tag{9}$$

and that for the annulus can be written as

$$v(y_2)\frac{\partial\theta_2}{\partial x}=\left(\frac{\Delta}{\Delta y_2-1}\right)\frac{\partial\theta_2}{\partial y_2}+\frac{\partial^2\theta_2}{\partial {y_2}^2};\qquad 0\leq y_2\leq 1,\quad 0\leq x\leq L \tag{10}$$

where

$$v(y_2)=\frac{KH\Delta}{(2-\Delta)}\left\{\frac{\Delta^2y_2^2+\Delta(2-\Delta)\dfrac{\ln(1-\Delta y_2)}{\ln(1-\Delta)}-2\Delta y_2}{2(1-\Delta)+\Delta^2+\dfrac{\Delta(2-\Delta)}{\ln(1-\Delta)}}\right\}$$

Experimentally, the assumption of fully developed flow can be approximated to any desired accuracy, within the limits of velocity variations caused by physical property variations, by having the thermal test section preceded by an isothermal section in which the parabolic velocity profile is established. However, if the system is arranged so that the entrance velocity profiles are flat, then the local Nusselt numbers would be somewhat high near the ends of the exchanger than those reported here. On the basis of single-stream calculations, one would expect the local results for these two cases to be essentially the same at dimensionless distances from the ends on the order of 0.04. Thus, if the exchanger is reasonably long, then overall behavior would not be markedly affected by the velocity entrance condition employed.

To reduce the number of parameters involved, it is assumed that no heat is transferred across the outer boundaries and that each stream enters with a uniform temperature profile. These assumptions, which are not essential to the development of the theory, lead to

$$\theta_1(0,y_1)=0 \tag{11}$$

$$\theta_2(L,y_2)=1 \tag{12}$$

$$\frac{\partial\theta_2}{\partial y_2}(x,0)=0;\qquad \frac{\partial\theta_1}{\partial y_1}(x,0)=0 \tag{13}$$

$$\frac{\partial\theta_2}{\partial y_2}(x,1)=-\frac{K\Delta}{(1-\Delta)}\frac{\partial\theta_1}{\partial y_1}(x,1) \tag{14}$$

$$\theta_2(x,1)=\theta_1(x,1)+K_w\frac{\partial\theta_1}{\partial y_1}(x,1) \tag{15}$$

Separation of variables in the form

$$\theta_i(x,y_i)=X_n(x)\,Y_{in}(y_i) \tag{16}$$

applied to Equations (9) and (10) leads to

$$X_n(x)=\exp(-\lambda_n x);\quad 0\leq x\leq L \tag{17}$$

$$y_1Y_{1n}''(y_1)+Y_{1n}'(y_1)+\lambda_n y_1(1-y_1^2)\,Y_{1n}(y_1)=0;\quad 0\leq y_1\leq 1 \tag{18}$$

$$\left(y_2-\frac{1}{\Delta}\right)Y''_{2n}(y_2)+Y'_{2n}(y_2)+\lambda_n\left(y_2-\frac{1}{\Delta}\right)v(y_2)\,Y_{2n}(y_2)=0;\quad 0\leq y_2\leq 1 \tag{19}$$

$$Y'_{1n}(0)=0 \tag{20}$$

$$Y'_{2n}(0)=0 \tag{21}$$

$$Y'_{2n}(1)=-\frac{K\Delta}{(1-\Delta)}Y'_{1n}(1) \tag{22}$$

$$Y_{2n}(1)=Y_{1n}(1)+K_wY'_{1n}(1) \tag{23}$$

where the primes on $Y_{1n}(y_1)$ and $Y_{2n}(y_2)$ refer to differentiation with respect to y_1 and y_2, respectively. The eigenfunction corresponding to λ_j is given by Y_{1j} in the region of stream 1 and by Y_{2j} in the region of stream 2. Equations (22) and (23) are the linking conditions for the two regions. Thus for a given value of the subscript n, Equations (18) and (19) describe the variation of a single function. Note that although conditions are written at the inner wall, the temperature and flux distributions there remain to be calculated.

It has been shown by the authors that Equation (26) is the orthogonality condition for the concentric tube heat exchanger.

$$\int_0^1 y_1(1-y_1^2)\,Y_{1j}(y_1)\,Y_{1m}(y_1)\,dy_1-\frac{1}{K}\int_0^1\left(y_2-\frac{1}{\Delta}\right)v(y_2)\,Y_{2j}(y_2)\,Y_{2m}(y_2)\,dy_2=0;\quad j\neq m \tag{26}$$

Note that the eigenfunctions are orthogonal with respect to the weighting function given by

$$\text{W.F.}=\begin{cases}y_1(1-y_1^2);\quad 0\leq y_1\leq 1\\ -\dfrac{1}{K}\left(y_2-\dfrac{1}{\Delta}\right)v(y_2);\quad 0\leq y_2\leq 1\end{cases} \tag{27}$$

and that the weighting function is positive in region 1 and negative in region 2.

Thus, for counterflow systems it is necessary to find a convergent series in both positive and negative eigenvalues, since each set must be retained if the orthogonal expansion is to be complete and the inlet conditions are to

be satisfied. In both single-stream and cocurrent flow systems, only one set of eigenvalues is necessary. This difference is a consequence of the difference in velocity profiles between problems as discussed in the Introduction and illustrated in Figure 1.

The solution for countercurrent flow can now be written as

$$\theta_i(x, y_i) = \sum_{n=0}^{\infty} B_n^+ X_n^+(x)\, Y_{in}^+(y_i) + \sum_{n=0}^{\infty} B_n^- X_n^-(x)\, Y_{in}^-(y_i) \quad ; \; i = 1, 2 \qquad (28)$$

which will be written here as simply

$$\theta_i(x, y_i) = \sum_n B_n X_n(x)\, Y_{in}(y_i) \quad ; \; i = 1, 2 \qquad (29)$$

General expressions for the expansion coefficients have been derived and finally culminate in Equation (38)

$$\int_0^1 y_1 (1 - y_1^2)\, \phi_1(y_1)\, Y_{1n}(y_1)\, dy_1 + \frac{1}{KX_n(L)} \int_0^1 \left(y_2 - \frac{1}{\Delta}\right) v(y_2)\, \psi_2(y_2)\, Y_{2n}(y_2)\, dy_2 = \sum_q B_q \left[\frac{X_q(L)}{X_n(L)} \int_0^1 y_1 (1 - y_1^2)\, Y_{1n}(y_1)\, Y_{1q}(y_1)\, dy_1 + \frac{1}{K} \int_0^1 \left(y_2 - \frac{1}{\Delta}\right) v(y_2)\, Y_{2n}(y_2)\, Y_{2q}(y_2)\, dy_2\right] \qquad (38)$$

Equation (38) applies for all values of n for both positive and negative eigenvalues and therefore constitutes a set of linear equations which defines the expansion coefficients.

Thus to find the expansion coefficients a set of simultaneous equations must be solved, and each successive term added to the expansion has an effect on the preceding expansion coefficients. This is not the case in single-stream and cocurrent flow systems, where each expansion coefficient is uniquely determined by the properties of the eigenfunction with which it is associated, and is a direct consequence of the differences in boundary conditions as discussed in the Introduction and illustrated in Figure 2.

It is interesting to note that Equation (38) reduces to the cocurrent flow expression as $L \to 0$. With the orthogonality condition for cocurrent flow, Equation (57), and $L = 0$, the right-hand side of Equation (38) is zero unless $q = n$. Thus

$$\int_0^1 y_1 (1 - y_1)\, \phi_1(y_1)\, Y_{1n}(y_1)\, dy_1 + \frac{1}{K} \int_0^1 \left(y_2 - \frac{1}{\Delta}\right) v(y_2)\, \psi_2(y_2)\, Y_{2n}(y_2)\, dy_2 = B_n \left[\int_0^1 y_1 (1 - y_1^2) Y_{1n}^2\, dy_1 + \frac{1}{K} \int_0^1 \left(y_2 - \frac{1}{\Delta}\right) v(y_2)\, Y_{2n}^2\, dy_2\right]$$

where $\phi_1(y_1)$ and $\psi_2(y_2)$ are the prescribed inlet conditions for streams 1 and 2, respectively. For $\phi_1 = 0$ and $\psi_2 = 1$, this reduces to Equation (60), the expression for the expansion coefficients in cocurrent flow.

Standard simplifying techniques using Equation (18) to (23) are employed to obtain expressions for the integrals in Equation (38). Thus for $\lambda_0 \neq 0$, Equation (38) becomes

$$\frac{-Y'_{2n}(1)}{\lambda_n \mathcal{N}_n(L)} = \sum_q B_q \begin{cases} \left[\dfrac{Y_{2n}(1)\, Y'_{2q}(1) - Y_{2q}(1)\, Y'_{2n}(1)}{\lambda_n - \lambda_q}\right] \left[1 + \dfrac{X_q(L)}{X_n(L)}\right] & ; \; q \neq n \\ 2Y'_{2n}(1) \dfrac{\partial Y_{2n}}{\partial \lambda_n}(1) - 2Y_{2n}(1) \dfrac{\partial Y'_{2n}}{\partial \lambda_n}(1) + \left(\dfrac{1}{1 - \Delta}\right) Y_{2n}(0) \dfrac{\partial Y'_{2n}}{\partial \lambda_n}(0) & ; \; q = n \end{cases} \qquad (39)$$

and for $\lambda_0^+ = 0$

$$H = (H + 1)\, B_0^+ + \frac{4(1 - \Delta)}{K\Delta} \sum_{q=1}^{\infty} B_q^+ \frac{Y_{2q}^+(1)}{\lambda_q^+} (1 + X_q^+(L)) + \frac{4(1 - \Delta)}{K\Delta} \sum_{q=0}^{\infty} B_q^- \frac{Y_{2q}^-}{\lambda_q^-} (1 + X_q^-(L)) \qquad (40)$$

If $\lambda_0^- = 0$, the + and − superscripts in Equation (40) are interchanged.

NUMERICAL CALCULATION OF EIGENVALUES AND RELATED QUANTITIES

To generate eigenvalues and related quantities an iterative numerical integration procedure was used. As in more conventional Sturm-Liouville problems, the eigenvalues are determined such that $Y'_{1n}(0) = 0$, and the eigenvectors compensate for any chosen value of $Y_{1n}(0)$. Therefore, without loss of generality it can be assumed that

$$Y_{1n}(0) = 1 \qquad (41)$$

The general scheme for solving the system of Equations (18) to (23) is as follows:

1. Assume an approximate value for the eigenvalue.
2. Starting with the conditions $Y_{1n}(0) = 1$ and $Y'_{1n}(0) = 0$, integrate Equation (18) from $y_1 = 0$ to $y_1 = 1$. Then introduce Equations (22) and (23) and integrate Equation (19) from $y_2 = 1$ to $y_2 = 0$.
3. Repeat step 2 with some multiple of the first approximation to the eigenvalue.
4. Calculate a better approximation to the eigenvalue by using the results of the previous integrations and test the difference between approximations against a preassigned allowable error. If the difference is less than the error, go to step 6; if the difference is greater than the error, go to step 5.
5. Repeat steps 2 and 4 with the new approximation.
6. Calculate quantities associated with the eigenvalue by a final integration and then return to step 1.

The techniques used for carrying out these steps were a fourth-order Runge-Kutta numerical integration (13) and a false position iteration. To solve for the expansion coefficients, a Gauss-Jordan pivotal reduction was used. Calculations were made on an IBM 7074 computer.

Several sets of parameters for the concentric tube problem have been investigated using these techniques. Table 1* lists the eigenvalues and related quantities and Table 2* the expansion coefficients. The properties of the eigenfunctions are illustrated in Figure 4, which shows that the positive eigenfunctions are periodic in the region of posi-

* See footnote on page 279.

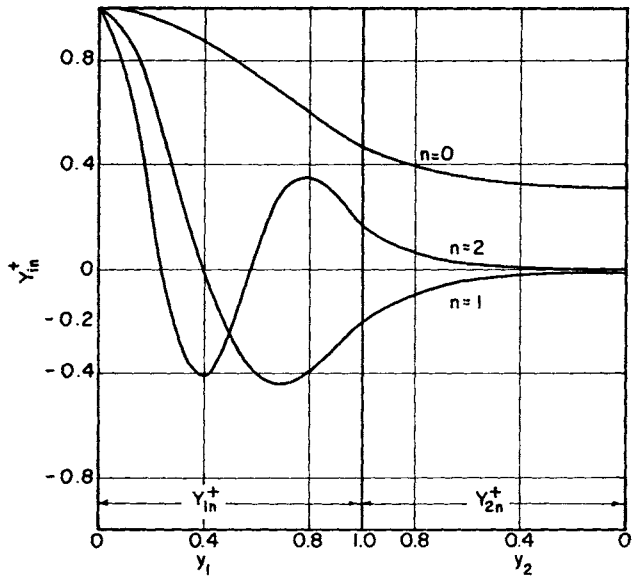

Fig. 4. Positive eigenfunctions for a counterflow concentric tube heat exchanger with $H = 2.25$, $K = 0.6$, $K_w = 0$, and $\Delta = 0.5$.

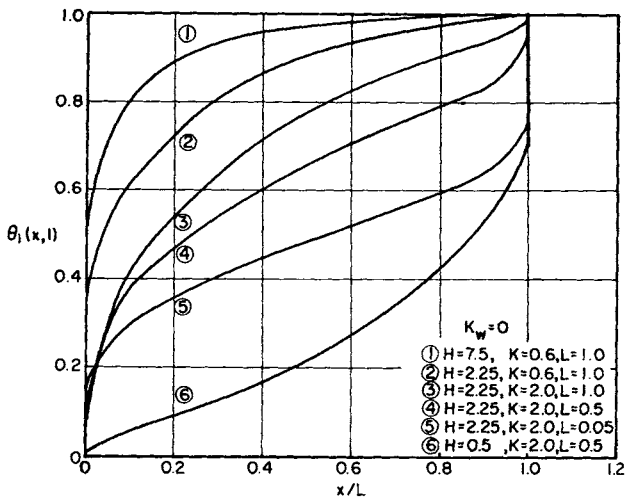

Fig. 5. Temperature distribution at the wall-fluid interface for several sets of parameters in a concentric tube heat exchanger.

tive velocity. Similarly, the negative eigenfunctions are periodic in the region of negative velocity as required by Sturm's comparison theorem. Furthermore, this is intimately related to the approximation of the entrance conditions. The addition of more negative terms improves the fit in the region of negative velocity, while the addition of more positive terms has a similar effect in the region of positive velocity.

LOCAL BEHAVIOR IN COUNTERFLOW SYSTEMS

One of the interesting results for counterflow exchangers is the temperature distribution of the wall-fluid interface for each of the two streams. If the wall between the two streams is very thin, or if $k_w >> k_1$, then $K_w = 0$ is a reasonable assumption. The temperature distribution of the wall-fluid interface is then the same for both streams and should vary between 0 at $x = 0$ and 1 at $x = L$. Figure 5 illustrates the variety of distributions which is possible as the values of the parameters are changed. Rapid changes are indicative of a large heat flux and, correspondingly, small changes such as for curve 1 near $x/L = 1$ designate a region where the flux is small. Curves such as the last are characteristic of the distribution obtained when the outlet temperature of stream 1 approaches the inlet of stream 2, or in the case of curve 6, when the outlet temperature of stream 2 approaches the inlet temperature of stream 1.

When a wall resistance is present, the interfacial wall-fluid temperature distributions are no longer identical for each stream. However, the results for $K_w = 0$ are contained between those having resistance for the same values of the other parameters. As K_w increases the distributions are shifted farther apart. When $K_w \neq 0$, the heat flux at each end of the exchanger is smaller than that for $K_w = 0$, and the changes in the temperature distribution at the wall near the ends are also reduced.

The behavior of the local Nusselt numbers is a particularly important result which is provided by the orthogonal expansion solution. The local Nusselt number for each stream is defined by

$$N_{Nu_i}(x) = \frac{h_i(x)d_i}{k_i} = \frac{-2\dfrac{\partial\theta_i}{\partial y_i}(x,1)}{\theta_{iB}(x) - \theta_i(x,1)} \qquad (42)$$

and an overall Nusselt number, arbitrarily based on the properties of stream 1, is given by

$$N_{Nu_0}(x) = \frac{U(x)d_1}{k_1} = \frac{-2\dfrac{\partial\theta_1}{\partial y_1}(x,1)}{\theta_{1B}(x) - \theta_{2B}(x)} \qquad (43)$$

where d_i is the hydraulic equivalent diameter. With these definitions the relations between the local values of the overall and individual Nusselt numbers based on the inside tube diameter

$$\frac{1}{N_{Nu_0}(x)} = \frac{1}{N_{Nu_1}(x)} + \frac{K\Delta}{(1-\Delta)}\frac{1}{N_{Nu_2}(x)} + \frac{K_w}{2} \qquad (44)$$

agree with the dimensionless form of the additivity of resistance concept.

From these definitions and the form of the solution,

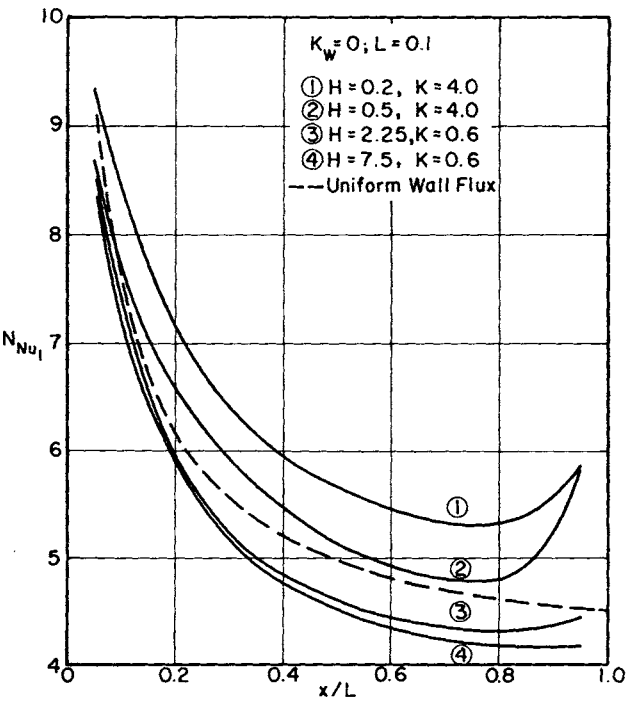

Fig. 6. Local Nusselt numbers for the tube-side stream in a concentric tube heat exchanger compared to the local Nusselt number for UWF in single-stream flow.

Equation (28), expressions for the local Nusselt numbers are derived. Thus, for the tube

$$N_{Nu_1}(x) = \frac{-2\dfrac{(1-\Delta)}{K\Delta}\left\{\sum_{n=1}^{\infty} B_n^+ X_n^+(x) Y_{2n}^{+\prime}(1) + \sum_{n=0}^{\infty} B_n^- X_n^-(x) Y_{2n}^{-\prime}(1)\right\}}{\sum_{n=1}^{\infty} B_n^+ X_n^+(x) Z_n^+ + \sum_{n=0}^{\infty} B_n^- X_n^-(x) Z_n^-} \tag{45}$$

where

$$Z_n^{\pm} = Y_{2n}^{\pm}(1) - \frac{(1-\Delta)}{K\Delta}\left\{K_w - \frac{4}{\lambda_n^{\pm}}\right\} Y_{2n}^{\pm}(1)$$

and the annulus result is

$$N_{Nu_2}(x) = \frac{2\left\{\sum_{n=1}^{\infty} B_n^+ X_n^+(x) Y_{2n}^{+\prime}(1) + \sum_{n=0}^{\infty} B_n^- X_n^-(x) Y_{2n}^{-\prime}(1)\right\}}{\sum_{n=1}^{\infty} B_n^+ X_n^+ S_n^+ + \sum_{n=0}^{\infty} B_n^- X_n^- S_n^-} \tag{46}$$

where $$S_n^{\pm} = Y_{2n}^{\pm}(1) - \frac{4(1-\Delta)}{KH\Delta}\frac{Y_{2n}^{\pm\prime}(1)}{\lambda_n^{\pm}}$$

The boundary conditions of uniform wall temperature and uniform heat flux have been used for single-stream problems, since under certain conditions they resemble the individual streams in the counterflow exchanger. The single-stream problems of uniform wall flux (UWF) (*16*), and uniform wall temperature (UWT) (*14*), for fully developed velocity profiles can be compared with the results for the tube in the counterflow exchanger. When these comparisons are made consistent trends are found. Figure 6 shows some of the results for concentric tubes along with the UWF results. As indicated in Figure 6 the UWF divides the results for various values of H; for $H > 1$, the local Nusselt numbers are less than the UWF results and for $H < 1$ above it. Figure 6 also shows that H has a greater effect on the variation of the local Nusselt number below 1 than above it. Except near the exit, for the case $H < 1$, the UWF results are generally within $\pm 20\%$ of the local results calculated here.

However, the increase in the individual Nusselt number near the exit is not predicted by the results for single-stream flow. End effects are especially pronounced for small L, large K, and $H < 1$. Verification of this behavior in counterflow systems has been obtained by finite-difference solutions both here and in King's (*8*) work on mass transfer. Physically, this can be explained by the high transfer rates which occur in the regions near the inlets for each stream. The large flux carries over to the exiting stream with a resultant increase in the Nusselt number. When $K_w \neq 0$, the heat flux at the ends is reduced and, in turn, these end effects are dampened.

The value of K_w has only a small effect on the individual Nusselt numbers, except near the ends of the exchanger as described above. However, the local behavior depends markedly on the values of the parameters K, H and L. At constant L and K, Figure 6 shows that as H decreases, the $N_{Nu_1}(x)$ curve is shifted upward, while at constant L and H with $H > 1$, increases in K result in a decrease in $N_{Nu_1}(x)$. For $H < 1$ increases in K result in an increase in $N_{Nu_1}(x)$. If the parameters are redefined with respect to stream 2 such that

$$H_2 = 1/H,\ K_2 = 1/K,\ K_{w_2} = \frac{K_{w_1}}{K}\left(\frac{1-\Delta}{\Delta}\right),\ \Delta_2 = 1-\Delta$$

and

$$L_2 = \frac{L(1-\Delta)}{KH\Delta}$$

then the same trends hold true for stream 2. Increases in L with the other parameters constant decrease the local Nusselt numbers for both streams.

ASYMPTOTIC BEHAVIOR IN COUNTERFLOW SYSTEMS

Consideration of the local behavior of the Nusselt numbers showed that as L increased, the Nusselt numbers decreased. Closer examination reveals that the local values decrease to a certain value and no lower, no matter how large L is made. This lower bound, which depends on H, K, and K_w but not on L, can be termed an asymptotic value. However, it is important to note that the asymptotic region occurs near the center of the exchanger rather than at the ends. As illustrated in Figure 7 this region takes up an increasing percentage of the total exchanger as L increases. Expressions for the asymptotic Nusselt numbers are derived from the expressions for the local Nusselt numbers given by Equations (45) and (46) by dropping all but the zeroth-order terms. When $\lambda_0^+ = 0$, these expressions are

$$N_{Nu_1} = \frac{-2\dfrac{(1-\Delta)}{K\Delta}Y_{20}^{-\prime}(1)}{Y_{20}^{-}(1) + \dfrac{(1-\Delta)}{K\Delta}\left[K_w - \dfrac{4}{\lambda_0^-}\right]Y_{20}^{-\prime}(1)} \tag{47}$$

$$N_{Nu_2} = \frac{2Y_{20}^{-\prime}}{Y_{20}^{-}(1) - \dfrac{4}{KH}\dfrac{(1-\Delta)}{\Delta}\dfrac{Y_{20}^{-\prime}(1)}{\lambda_0^-}} \tag{48}$$

$$N_{Nu_0} = \left(\frac{H}{H-1}\right)\frac{\lambda_0^-}{2} \tag{49}$$

When $\lambda_0^- = 0$, the negative superscripts are replaced by positive ones. It is important to note that these expressions are independent of the expansion coefficients. Also, they require a knowledge of only quantities related to the zeroth-order eigenvalues and, therefore, require a minimum of computation time. Thus the eigenfunction expansion is a particularly powerful tool of analysis for describing the asymptotic region, which is of considerable practical important, particularly when one wishes to effect large temperature changes in the streams and thereby requires a long exchanger.

Frequently the annular space is approximated by the space between parallel plates to remove the radius ratio Δ as a parameter. This approximation, which holds when the annular space is very narrow and Δ approaches zero, was employed to establish limiting results in the asymp-

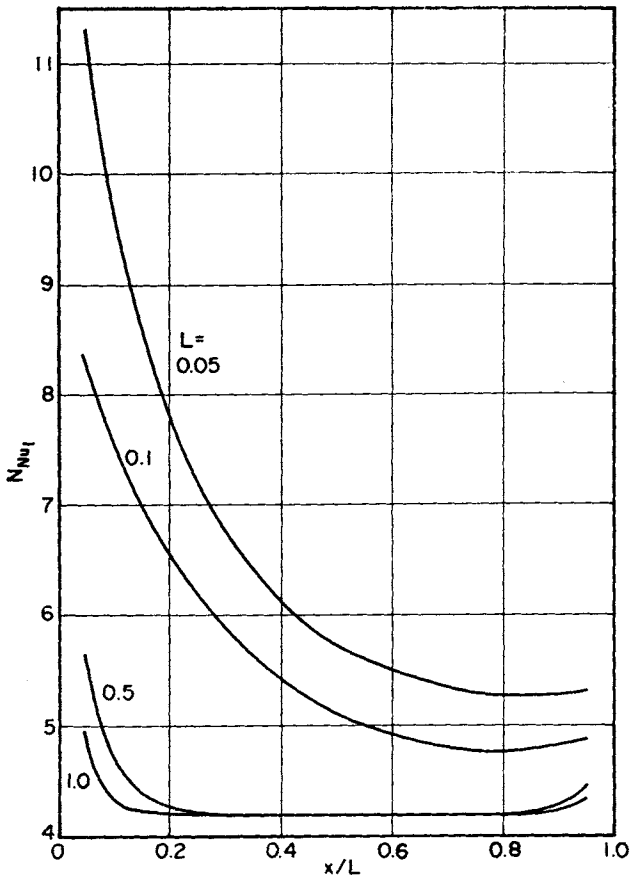

Fig. 7. Local Nusselt numbers in a concentric tube heat exchanger illustrating the effect of L with $H = 2.25$, $K = 2.0$, $K_w = 0$, and $\Delta = 0.5$.

totic region. In this case Equation (10) for the annular space is replaced by

$$\left[\frac{3}{2}\left(\frac{K\Delta}{1-\Delta}\right)Hy_2\,(y_2-1)\right]\frac{\partial\theta_2}{\partial x}=\frac{\partial^2\theta_2}{\partial y_2{}^2} \qquad (50)$$

in the model given by Equations (9) to (15). Now, K and Δ are not separate parameters but are combined to form the single parameter, $\frac{K\Delta}{1-\Delta}$. The asymptotic Nusselt numbers are given by Equations (47) to (49).

The usefulness of asymptotic values in design is limited to problems in which a high effectiveness for the exchanger is desired, since only then are the local Nusselt numbers relatively constant over the entire exchanger (the effectiveness increases as L increases and, as discussed previously as L increases the local Nusselt numbers approach the asymptotic values). However, this is very often the case in industrial applications, and for turbulent systems, in which the asymptotic result is obtained in identical fashion; the asymptotic result also will be of primary importance. Since the asymptotic values represent a lower limit, underdesign would never be a problem, but exchangers could be seriously overdesigned. For example, if asymptotic results were used to design an exchanger with $H = 2.25$, $K = 2.0$, $\Delta \neq 0.5$, and $K_w = 0$ having an effectiveness of 35% for heating the cold fluid, the predicted L from Equation (53), which is given in the section on overall results, would be, with $N_{Nu0m} = 1.83$

$$L=\frac{0.35}{2(1.83)\left(\dfrac{0.35-0.155}{\ln\dfrac{0.845}{0.65}}\right)}=0.130$$

Table 3. Asymptotic Nusselt Numbers for Single-Stream Flow with the Boundary Conditions of Uniform Wall Flux and Uniform Wall Temperature

Configuration	$N_{Nu}=\frac{hd}{k}$ UWF	UWT
Tube (*16*)	4.36	3.65
Parallel plates, one side insulated (*5*)	5.38	4.86
Annular space, one side insulated (*5*)		
$\Delta = 0.833$	9.22	8.87
$\Delta = 0.5$	6.18	5.74

while the actual calculation indicates $L = 0.1$ is sufficient. However, at an effectiveness of 93%, the predicted L is less than 3% greater than the calculated L.

Because of the ease of calculation, asymptotic results present an easy method of investigating a large number of different systems, and, when these results are used in conjunction with the local variation, trends of behavior in counterflow heat transfer systems can be established.

Frequently, it is suggested that the results for single-stream problems can be applied to cocurrent and countercurrent flow heat exchangers, at least to establish limiting transfer rates. Two of the most common boundary conditions considered are the uniform wall temperature and uniform wall flux cases. To test the applicability of these results to counterflow exchangers, the asymptotic Nusselt numbers obtained here have been normalized with respect to UWF and also compared with the UWT Nusselt numbers listed in Table 3. Table 4* gives the asymptotic Nusselt numbers and the quantities necessary to calculate them. Stein (*17*) made a similar investigation in a cocurrent flow exchanger and found that the UWF result was an upper bound for his asymptotic results, but that the lower limit approached zero, considerably below the UWT result. For counterflow exchangers the Nusselt numbers obtained here show that the UWT is a lower bound, but that under certain conditions, which are not unrealistic in a practical sense, the Nusselt numbers can exceed those for UWF substantially.

As discussed previously, UWF divides the local results for $H < 1$ and $H > 1$, with the Nusselt numbers for $H > 1$ falling below UWF. Asymptotically, this same phenomenon is observed and if the results at constant K, K_w, and Δ for H above and below 1 are joined by a smooth curve, the curve passes through the UWF result at $H = 1$. Coupling this with the local results, it is highly probable that the case $H = 1$ closely approximates the UWF be-

* See footnote on page 279.

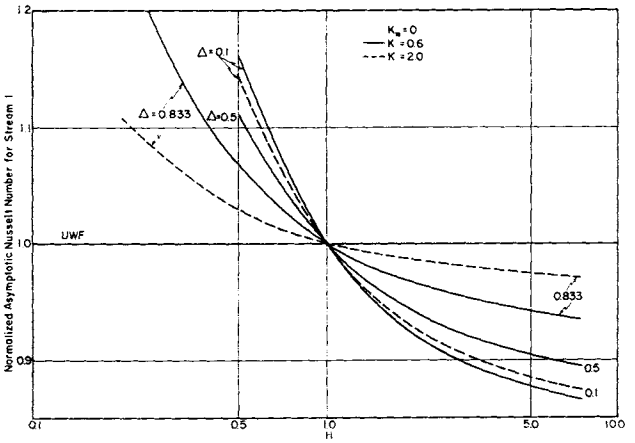

Fig. 8. Normalized asymptotic Nusselt numbers vs. H for the tube-side stream in a concentric tube heat exchanger.

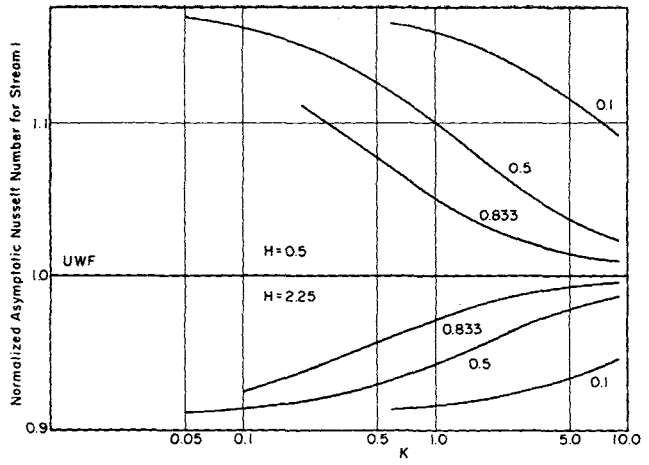

Fig. 9. Normalized asymptotic Nusselt numbers vs. K for the tube-side stream in a concentric tube heat exchanger with H and Δ as parameters and $K_w = 0$.

havior locally as well as asymptotically. (This could not be established with complete certainty, since the orthogonal function expansion is not applicable for $H = 1$.)

Figures 8 through 13 show the variation of asymptotic Nusselt numbers for the tube-side stream with H, K, Δ, and K_w, and illustrate several general trends. Figure 8 shows that as H approaches zero, the normalized Nusselt numbers apparently increase without bound. As H goes to infinity, the N_{Nu} approach a constant value between UWF and UWT, which is lowest for $\Delta = 0.1$ and closest to UWF for $\Delta = 0.833$. Comparison of the curves for constant Δ in Figure 8 shows that K has only a small effect on results for $\Delta = 0.1$, but that as Δ increases, larger values of K keep the N_{Nu} closer to UWF. Figures 9 and 10 show that as K approaches infinity, all asymptotic values approach that for UWF, the curves for $H > 1$ from below and for $H < 1$ for above. As K approaches zero, the N_{Nu} approach a constant value between UWF and UWT which is dependent on H, since as H decreases below 1, the constant value increases and as H increases above 1, the value decreases. However, this constant value is not dependent on Δ and, therefore, suggests that the data might be better correlated by a parameter containing both K and Δ.

To compare the results of the parallel plate approximation to those for the annular space where Δ is a parameter,

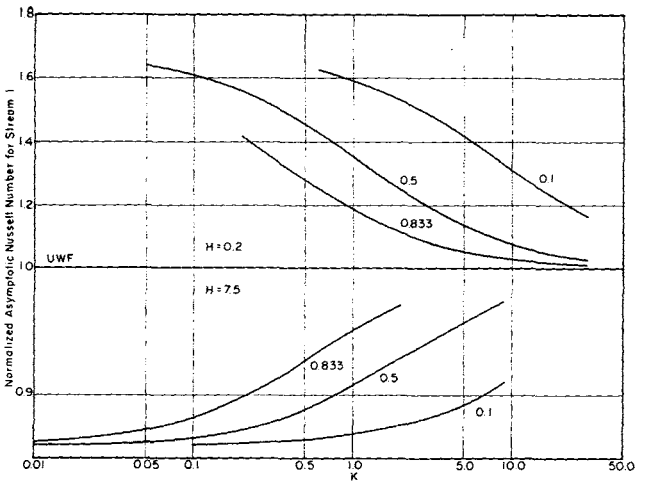

Fig. 10. Normalized asymptotic Nusselt numbers vs. K for the tube-side stream in a concentric tube heat exchanger with H and Δ as parameters and $K_w = 0$.

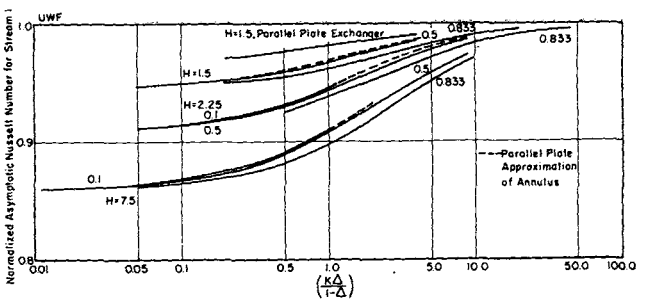

Fig. 11. Normalized asymptotic Nusselt numbers vs. $[K\Delta/(1-\Delta)]$ for the tube-side stream in a concentric tube heat exchanger with H and Δ as parameters, $H>1$ and $K_w = 0$.

the parameter $\left(\frac{K\Delta}{1-\Delta}\right)$ can be used. Figure 11 shows that for $H > 1$ the curves for all values of Δ and for the parallel plate approximation are very close together. For $H < 1$ in Figure 12, however, the results are not nearly as close together, especially at $H = 0.2$. In both Figures 11 and 12 the curves for $\Delta = 0.1$, and those for the parallel plate approximation coincide. The data for the parallel plate exchanger are included in both Figures 11 and 12 for comparison and are, in general, closer to those for UWF than are the tube results at the same values of the parameters.

Figure 13 illustrates the effect of K_w on the asymptotic values with all results approaching UWF as K_w increases. Curves 4, 5, and 6 in Figure 13 show that the influence of K_w decreases as Δ increases. A comparison of curves 1 and 3 shows that K_w has less influence as H approaches 1. That K_w also has less influence as K increases is evident upon comparing curves 2, 3, 7 and 8.

If the parameters are redefined with respect to the annular space, the same general trends for H, K, Δ, and K_w hold as is evident in Figure 14. However, plotting the Nusselt numbers vs. $\frac{(1-\Delta)}{K\Delta}$ or $\frac{K_2\Delta_2}{1-\Delta_2}$ does not correlate the data of the annulus as it did for the tube.

The asymptotic Nusselt numbers can be used to establish which sets of parameters lead to a controlling resistance to heat transfer. Considering arbitrarily that if N_{Nu_0} is 95% of one term in the additivity of resistance equation then that resistance is controlling, the limits given in Table 5, which are essentially independent of H, can be

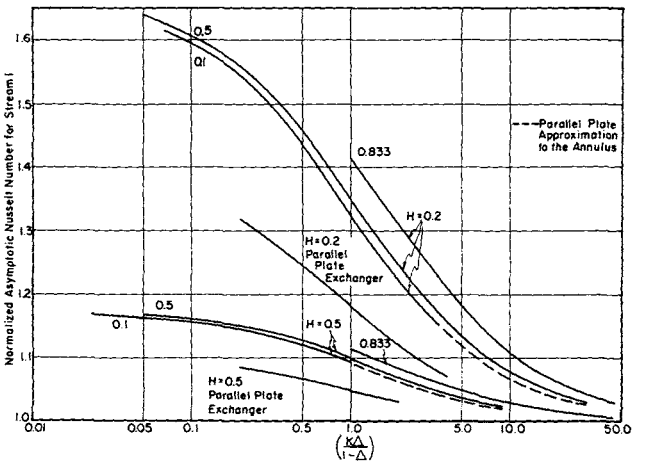

Fig. 12. Normalized asymptotic Nusselt numbers vs. $[K\Delta/(1-\Delta)]$ for the tube-side stream in a concentric tube heat exchanger with H and Δ as parameters, $H<1$ and $K_w = 0$.

established. For example, with $\Delta = 0.833$ and $K \geq 2$, the stream in the annulus controls and

$$N_{Nu0} \approx \frac{(1-\Delta)}{K\Delta} N_{Nu2}$$

The results for the parallel plate approximation can be applied to yield slightly better estimations for $\Delta = 0.1$. Thus the annulus controls when $K > 81$ and the tube-side stream controls for $K \leq 0.9$.

It appears from the discussion of the asymptotic behavior of the individual stream Nusselt numbers that in many cases the UWF result could be used to predict counterflow results with reasonable accuracy. The overall asymptotic Nusselt numbers can be used to investigate this possibility and to establish situations in which this approximation would lead to serious error. With the additivity of resistance concept and the single- stream values given in Table 3, a UWF overall asymptotic Nusselt number can be calculated and compared with those calculated by the method of this study. Table 6 gives the results of such a calculation. The cases in which the UWF is greater than that calculated here would yield a shorter length than is actually necessary, while when UWF result is less than the calculated Nusselt number the exchanger would be longer than necessary.

From the viewpoint that a conservative design is the lesser of two evils, the limits within which the UWF model are considered to predict counterflow system behavior are arbitrarily set at 10% less, or 3% greater, than the calculated result. Table 7 lists the results of this analysis. The lower limits for $H > 1$ mean that using UWF below this value yields an underdesigned exchanger, while the upper limit indicates an overdesigned exchanger, and the meaning of the limits is reversed for $H < 1$. For H near 1, the limits are much less stringent than for $H >> 1$ and $H << 1$. Some of the limits are quite indefinite, since values above and below those listed were not investigated. These limits cannot be strictly applied at local levels but serve to indicate where the local variation of the overall Nusselt number will probably be significantly different from that predicted by using the UWF model.

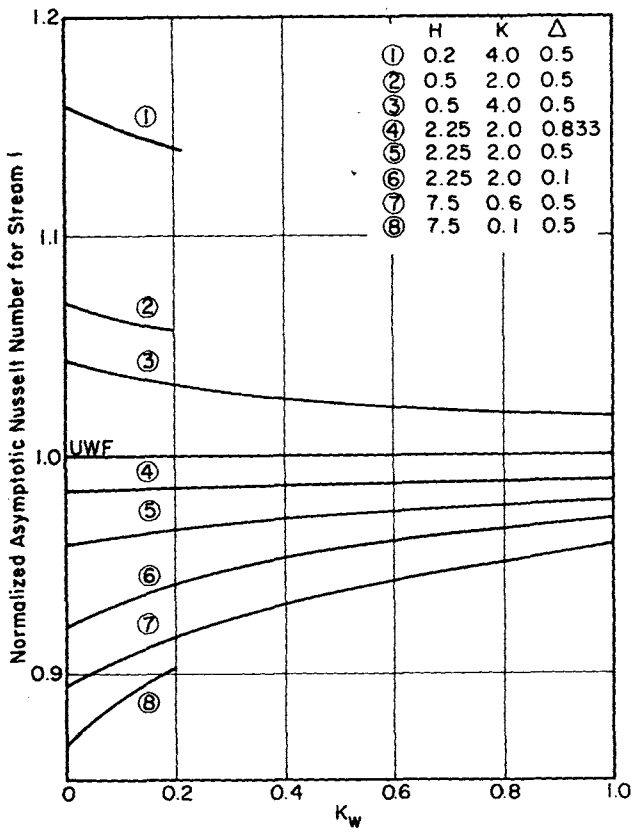

Fig. 13. Normalized asymptotic Nusselt numbers vs. K_w for the tube-side stream in a concentric tube heat exchanger.

OVERALL RESULTS FOR COUNTERFLOW HEAT TRANSFER

Design for laminar counterflow concentric tube exchangers is generally based on empirical correlations of experimental data. Kern (7) suggested the correlation of Sieder and Tate (15) for the Nusselt number

$$N_{Nua.m.} = 1.86 \left(\frac{l/d}{N_{Pe}}\right)^{-1/3} \left(\frac{\mu_B}{\mu_w}\right)^{0.14} \qquad (51)$$

be used for both the annulus and tube-side streams. $N_{Nua.m.}$ is an average Nusselt number based on the arithmetic mean of the terminal fluid temperatures. The equivalent diameter for the annulus is $2\left(\frac{r_2^2 - r_0^2}{r_0}\right)$ rather than $2b_2$ as in this study. Equation (51) correlates to $\pm 12\%$ the data of several experimenters for heat transfer to fluids in circular tubes with widely varying wall conditions. For example, Sieder and Tate used a counterflow exchanger with water as the annular fluid (but did not attempt to correlate the annulus heat transfer results); Kirkbride and McCabe (9) used a condensing steam heater approximating UWT; and Drew (4) used an electrically heated tube approximating UWF.

Most of the results correlated by Sieder and Tate were for petroleum fractions having large Prandtl numbers and high coefficients of viscosity, and their own experimental data cover a rather limited range when compared to the parameters used in this study. The list below indicates that only H was allowed to vary over any appreciable range.

$$0.2 < H < 5.5$$
$$K \approx 0.025$$
$$\Delta = 0.4$$
$$K_w = 0$$
$$0.001 \leq L \leq 0.005$$

Perhaps the most limiting condition in their work is the variation of L. In all theoretical investigations of Graetz types of problems the local Nusselt numbers approach an asymptotic value > 0. Obviously, the average value of the Nusselt number can never decrease below the asymptotic value. Equation (51) shows that the average Nusselt number approaches zero as L increases. Several theoretical results for differing wall conditions in single-stream flow can be correlated for (10)

$$\left(\frac{l/d}{N_{Pe}}\right) < 0.01$$

by the same exponent on the Graetz number as in Equation (51). However, if the correlation is extended beyond the limit, the Nusselt numbers are much lower than the calculated values. Thus it seems clear the Equation (51) was obtained in too limited a region and does not hold in general. Also, in view of the variations in asymptotic behavior in the annulus for different values of Δ, it appears that using this correlation for the annulus is too great a simplification. However, since Kern presents this correlation as a usable one for design, it is interesting to compare overall Nusselt numbers calculated by the method of this study and by those using Equation (51). Table 8 gives a comparison of the two results. The mean individual Nusselt numbers, calculated from Equation (52), provide a comparison for the Nusselt numbers calculated from Equation (51). It is evident that the Nusselt numbers for the tube are in fair agreement for the shorter lengths and lower efficiencies. However, the values for

Table 5. Limits of K or $\left(\frac{K\Delta}{1-\Delta}\right)$ for Assuming Heat Transfer Control by Either the Fluid in the Tube or in the Annulus of a Counterflow Concentric Heat Exchanger

Δ	K or $\left(\frac{K\Delta}{1-\Delta}\right)$	Controlling stream
Parallel plate approx.	>9	annulus
Parallel plate approx.	≤0.1	tube
0.1	>>30	annulus
0.1	<0.6	tube
0.5	>9	annulus
0.5	≤0.1	tube
0.833	≥2	annulus
0.833	<0.05	tube

Table 6. Asymptotic Overall Nusselt Numbers for Concentric Tube Heat Exchangers with UWF Boundary Condition for each Stream and $K_w = 0$

K	$\Delta = 0.833$	$\Delta = 0.5$	Parallel plate approx.
30.0	0.0607	0.197	0.171
9.0	0.196	0.591	0.527
4.0	0.416	1.14	1.03
2.0	0.762	1.81	1.67
1.0	1.30	2.56	2.68
0.6	1.80	3.06	2.93
0.2	2.97	3.83	3.77
0.1	3.53	4.08	4.03
0.05	3.91	4.20	4.18
0.01	4.27	4.33	4.32

Table 7. Limits of K or $\left(\frac{K\Delta}{1-\Delta}\right)$ for Predicting Asymptotic Nusselt Numbers for Counterflow Concentric Tube Heat Exchangers Using UWF Nusselt Numbers for Single-Stream Flow

	$\Delta = 0.833$		$\Delta = 0.5$		Parallel plate approximation	
H	Lower limit, K	Upper limit, K	Lower limit, K	Upper limit, K	Lower limit, $\left(\frac{K\Delta}{1-\Delta}\right)$	Upper limit, $\left(\frac{K\Delta}{1-\Delta}\right)$
7.5	>0.1	<2.0	>0.6	<9.0	>0.6	<2.0
2.25	0.6	>9.0	>0.6	>9.0	>0.6	>9.0
1.5	0.6	>9.0	0.6	>9.0	2.0	>4.0
0.5	<0.2	>9.0	0.6	4.0	>0.2	2.0
0.2	0.6	<4.0	>1.0	<4.0	>0.6	<4.0

Table 8. A Comparison of Mean Nusselt Numbers for Concentric Tube Heat Exchangers Calculated by the Orthogonal Expansion Technique and the Correlation of Sieder and Tate (15) with $H = 2.25$, $K = 2.25$, $K = 0.6$, $\Delta = 0.5$, and $K_w = 0$

L	L_2	$Nu_{1a.m.}$	$Nu_{2a.m.}$	Nu_0	Nu_{1m}	Nu_{2m}	Nu_{0m}	ϵ, %
0.05	0.111	6.37	3.40	3.00	6.25	8.05	4.05	31.2
0.10	0.222	5.06	2.70	2.39	5.28	7.14	3.54	46.4
0.50	1.11	2.95	1.57	1.39	4.34	6.58	3.06	89.0
1.00	2.22	2.35	1.25	1.08	4.15	6.23	2.98	97.9

To compare the results for stream 2, Equation (51) was restated in terms of the equivalent diameter used in this work. Thus

$$Nu_{2_{a.m.}} = 0.62\left(\frac{18}{L_2}\right)^{1/3}$$

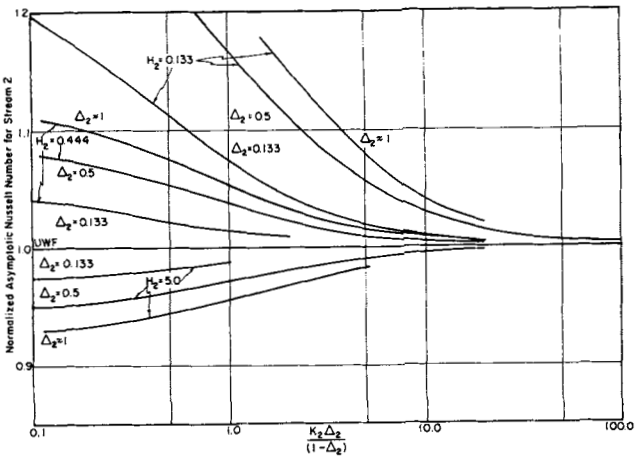

Fig. 14. Normalized asymptotic Nusselt numbers vs. $[K_2\Delta_2/(1-\Delta_2)]$ for the annulus with H_2 and Δ_2 as parameters.

the annulus at all L's and for the tube at larger L's do not agree and, therefore, the mean overall values do not agree. It appears from this calculation that Sieder and Tate's correlation gives reasonable results only for cases in which stream 1 controls and then only for an effectiveness of approximately 50% or less.

The overall results are listed in Table 9,* which also gives the comparison of mean overall Nusselt numbers calculated by Equations (52) and (53).

$$N_{Nu0m} = \frac{1}{L}\int_0^L N_{Nu_0}(x)\,dx \tag{52}$$

$$N_{Nu0m} = \frac{\theta_{1B}(L)}{2L\,\Delta\theta_{Bl.m.}} = \frac{H[1-\theta_{2B}(0)]}{2L\,\Delta\theta_{Bl.m.}} \tag{53}$$

The excellent agreement between the two calculations indicates a consistency in the results.

One of the most useful quantities calculated here is the variation with L of the bulk temperatures at the outlets of the exchanger. These data, plotted as effectiveness curves in Figures 15 and 16, specify the value of L neces-

* See footnote on page 279.

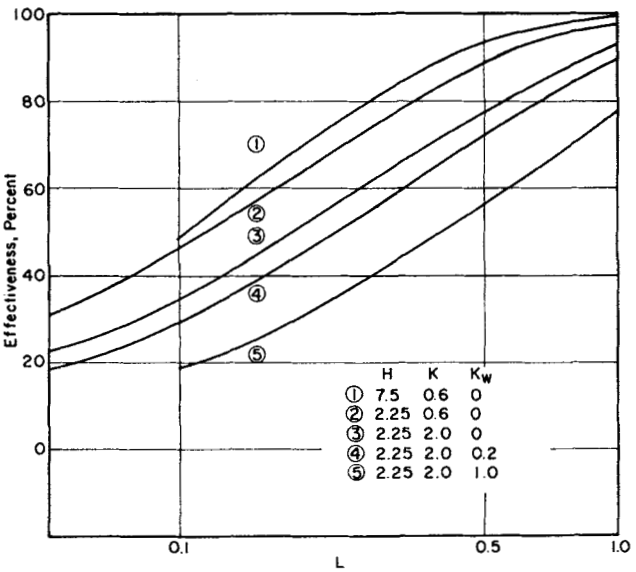

Fig. 15. The effectiveness of a counterflow concentric tube heat exchanger for heating the tube-side stream.

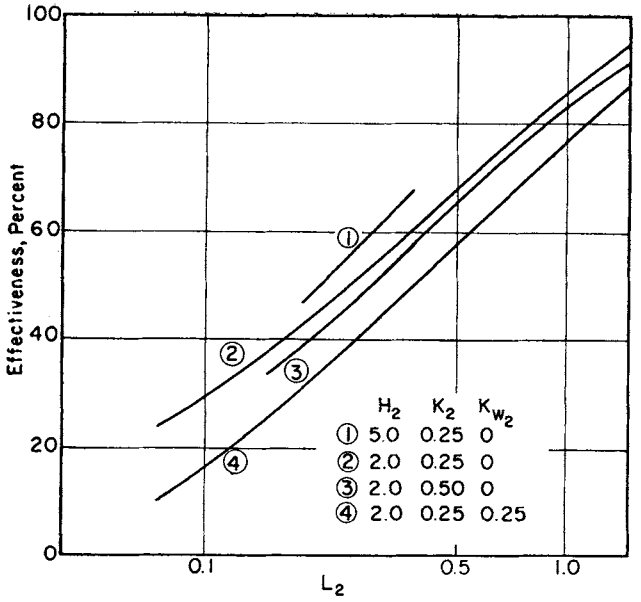

Fig. 16. The effectiveness of a counterflow concentric tube heat exchanger for cooling the stream in the annulus.

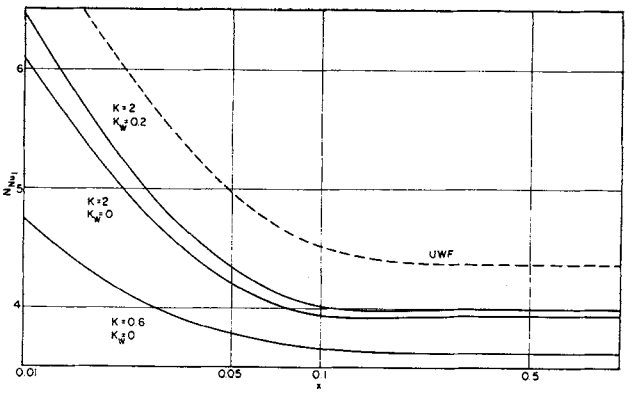

Fig. 17. Local Nusselt numbers for the tube-side stream of a cocurrent flow concentric tube heat exchanger with $\Delta = 0.5$ compared to the local Nusselt number for UWF in single-stream flow.

sary to obtain a desired temperature change as a function of the parameters H, K, and K_w. As discussed previously, when $H > 1$, ϵ measures the bulk temperature change in stream 1, while for $H < 1$, ϵ refers to stream 2. Upon redefining the parameters with respect to stream 2 and considering Figures 15 and 16, some general trends for the variation of the effectiveness with the parameters can be established. Large values of H or H_2 and small values of K or K_2 produce a higher effectiveness for a given length. It is also apparent that increases in K_w reduce the effectiveness significantly.

COCURRENT FLOW DOUBLE-PIPE HEAT EXCHANGER

The cocurrent flow double-pipe heat exchanger problem has been treated for laminar and plug flow by Stein (*17*). With the assumption that the annulus can be approximated by the space between infinite parallel plates, Stein developed an expression for the asymptotic Nusselt numbers. Here, to compare behavior in cocurrent and countercurrent flow systems, the cocurrent problem has been solved both to obtain inlet region results and to eliminate the parallel plate approximation. The numerical integration technique described previously provides an excellent means of finding eigenvalues and related quantities for this problem.

The mathematical model for cocurrent flow and its solution are given by Equations (54) to (60).* Equation (60) which is used to calculate the expansion coefficients is included here for comparison with a similar expression for countercurrent flow.

$$B_n = \frac{\frac{1}{K}\int_0^1 \left(y_2 - \frac{1}{\Delta}\right) v(y_2)\, Y_{2n}(y_2)\, dy_2}{\int_0^1 y_1(1-y_1^2)\, Y_{1n}^2(y_1)\, dy_1 + \frac{1}{K}\int_0^1 \left(y_2 - \frac{1}{\Delta}\right) v(y_2) Y_{2n}^2(y_2)\, dy_2} \qquad (60)$$

Eigenvalues, expansion coefficients, bulk temperatures and local Nusselt numbers for cocurrent flow are listed in Tables 10 and 11.*

An overall heat balance shows that with an infinite heat transfer area, the outlet temperature of each stream in cocurrent flow is

$$\theta_{i_B} = \frac{H}{H+1}$$

It is obvious then that the counterflow arrangement allows a greater maximum amount of heat transfer. However, it is not as obvious that the counterflow exchanger always yields a greater amount of heat transfer with the same parameters used for each exchanger. A comparison of the bulk temperature at the outlet for counterflow to the corresponding case for cocurrent flow indicates that the counterflow system does have a higher effectiveness. As explained by Bosworth (*3*), to get a highly efficient heat exchanger operation, the temperature of the colder body should be as little below the temperature of the hotter body as possible. Counterflow systems meet this requirement much better than do cocurrent flow arrangements.

Before concluding the discussion of cocurrent flow systems, it is worthwhile to consider the local variations of the individual stream Nusselt numbers. Stein found that the asymptotic Nusselt numbers were bounded by the UWF result for a single stream. Figure 17 illustrates that the local behavior is similar. However, it is noted that in each cocurrent flow problem solved the local variation of the Nusselt number for one of the two streams behaves in an unusual manner. In Figure 17, the Nusselt number for $K = 2.0$ decreases as x increases until a *minimum* is reached at $x \approx 0.15$ after which the Nusselt number then *increases* slightly to the asymptotic result. Hatton and Quarmby (*5*) encountered similar behavior for annuli with equal uniform heat inputs on each side, but offered no explanation. This effect does not seem to be intimately related to the value of H as so many characteristics of the counterflow system are, since it occurs in stream 1 for $H = 2.25$, $K = 2.0$ and in stream 2 for $H = 2.25$, $K = 0.6$. It appears that further investigation of this phenomenon is needed. For cocurrent plug flow, which involves a discontinuous weighting function, Stein (*18*) mentions a similar effect.

SUMMARY

Local Nusselt numbers, asymptotic Nusselt numbers, and bulk temperature changes for double-pipe heat exchangers have been predicted using certain simplifying

* See footnote on page 279.

assumptions. The variations of these quantities with the parameters H, K, K_w, L, and Δ have been investigated over a wide range of values of the parameters. The influence on the results of the neglected effects such as longitudinal axial conduction and temperature dependent fluid properties will be the subject of future studies.

It has been shown that the application of single-stream Nusselt number results to double-pipe exchangers is accurate only in a limited number of cases. Furthermore, a comparison of heat transfer coefficients from the correlation given by Sieder and Tate with those obtained here indicates that the use of this correlation for laminar flow is questionable in many situations.

The most useful numerical results, for design purposes, which are presented are the variation of the effectiveness with the parameters of the system. Larger values of H and the smaller values of K and K_w allow higher values of the effectiveness at the same length. Asymptotic Nusselt numbers, which effectively extend the range of results down to Graetz numbers of zero for very long exchangers and are of importance in applications requiring significant temperature changes, were obtained over a wider range of values of the parameters and can also be used for design when a large exchanger effectiveness is desired.

The orthogonal function method of solution given in this study can be used to solve a wide class of multiphase heat and mass transfer problems. In the traditional approach to single-stream flow heat transfer systems, the stream boundary conditions invariably involve a temperature, or temperature gradient, distribution which is arbitrarily specified in advance of solving the problem. Here, in contrast to traditional methods, both the temperature distribution of the separating surface and the rate of heat transfer between streams are determined as part of the solution to the stated problem. Thus, the present method accounts for coupling of heat transfer effects in the two phases.

ACKNOWLEDGMENT

This work was supported by the Office of Saline Water, U.S. Department of Interior. The numerical calculations were supported by NSF Grant GP 1137 to the Syracuse University Computing Center. This paper is based in part on studies carried out by the authors at Syracuse University which were related to the doctoral dissertation of R. J. Nunge.

NOTATION

B_n = expansion coefficient

b_i = width of stream i

b_w = wall thickness

C_{pi} = heat capacity of stream i

d_i = hydraulic equivalent diameter of stream i

H = dimensionless parameter, $\dfrac{w_2 C_{P2}}{w_1 C_{P1}}$

h_i = heat transfer coefficient in stream i

K = dimensionless parameter, k_1/k_2

K_w = dimensionless parameter, $\dfrac{k_1}{k_w} \ln (r_0/r_1)$

k_i = thermal conductivity of stream i

k_w = thermal conductivity of the wall

L = dimensionless parameter, $\dfrac{l}{N_{Pe1}\, b_1}$

l = length of exchanger

N_{Nui} = Nusselt number in stream i, defined by Equation (42)

N_{Nu0} = overall Nusselt number, defined by Equation (43)

N_{Nu0m} = mean overall Nusselt number defined by Equations (52) and (53)

N_{Pe} = Peclet number

r = radial coordinate

r_0 = $r_1 + b_w$

r_1 = inner radius of the inner tube in a concentric tube exchanger

r_2 = inner radius of outer tube in a concentric tube heat exchanger

T_0 = constant inlet temperature of stream 1

T_1 = constant inlet temperature of stream 2

u_i = bulk velocity of stream i

w_i = mass flow rate of stream i

x = dimensionless axial coordinate, $\dfrac{z}{N_{Pe1}\, b_1}$

Y_{in} = eigenfunction for stream i

y_i = dimensionless radial distance in stream i

z = axial distance

Greek Letters

α_i = $\dfrac{k_i}{\rho_i C_{pi}}$

Δ = dimensionless parameter, b_2/r_2

θ_i = dimensionless temperature or concentration of stream i, $(T_i - T_0)/(T_l - T_0)$

θ_{iB} = dimensionless bulk temperature of stream i

$\Delta\theta_{Bl.m.}$ = log mean temperature difference

λ_n = eigenvalue

μ_i = viscosity of stream i

ρ_i = density of stream i

ϵ = effectiveness

LITERATURE CITED

1. Bird, R. B., W. E. Stewart, and E. N. Lightfoot, "Transport Phenomena," Wiley, New York (1960).
2. Bocher, M., *Bull. Am. Math. Soc.*, **21**, 6 (1914).
3. Bosworth, R. C. L., and C. M. Groden, *Australian J. Phys.*, **17**, 26 (1964).
4. Drew, T. B., *Ind. Eng. Chem.*, **24**, 152 (1932).
5. Hatton, A. P., and A. Quarmby, *Intern. J. Heat Mass Transfer*, **5**, 973 (1962).
6. Ince, E. L., "Ordinary Differential Equations," Chapt. 10, Longsman-Green, London (1929).
7. Kern, D. Q., "Process Heat Transfer," Chapt. 6, McGraw-Hill, New York (1950).
8. King, C. J., *Ind. Eng. Chem. Fundamentals*, **4**, 125 (1965).
9. Kirkbride, C. G., and W. L. McCabe, *Ind. Eng. Chem.*, **23**, 625 (1931).
10. Knudsen, J. G., and D. L. Katz, "Fluid Dynamics and Heat Transfer," Chapt. 15, McGraw-Hill, New York (1958).
11. Nunge, R. J., and W. N. Gill, *Intern. J. Heat Mass Transfer*, **8**, 873 (1965).
12. ———, and R. P. Stein, *Ind. Eng. Chem. Fundamentals*, Res. Results Manuscript No. 263, submitted July, 1965.
13. Scarborough, J. B., "Numerical Mathematical Analysis," Chapt. 11, Johns Hopkins, Baltimore (1958).
14. Sellars, J. R., M. Tribus, and J. S. Klein, *Trans. Am. Soc. Mech. Engrs.*, **78**, 441 (1956).
15. Sieder, E. N., and G. E. Tate, *Ind. Eng. Chem.*, **8**, 1429 (1936).
16. Siegel, R., E. M. Sparrow, and T. H. Hallman, *Appl. Sci. Res.*, **A7**, 386 (1958).
17. Stein, R. P., *ANL-6889* (September, 1964).
18. ———, in "Advances in Heat Transfer," T. F. Irvine and J. P. Hartnett, ed., Vol. III, Academic Press, New York, to be published.

Manuscript received August 26, 1965; revision received October 27, 1965; paper accepted October 27, 1965. Paper presented at A.I.Ch.E. Philadelphia meeting.